Available online at www.sciencedirect.com
ScienceDirect
Biochemical and Biophysical Research Communications 351 (2006) 113–117
BBRC
www.elsevier.com/locate/ybbrc

Determining OMP topology by computation, surface plasmon resonance and cysteine labelling: The test case of OMPG

Virak Visudtiphole, David A. Chalton, Qi Hong, Jeremy H. Lakey *

Institute for Cell and Molecular Biosciences, University of Newcastle, Newcastle NE2 4HH, UK

Received 28 September 2006
Available online 10 October 2006

Abstract

Bacterial outer-membrane proteins (OMP) are important in pathogenicity and the recently solved structure of OmpG provides an excellent test case for topological predictions since it is monomeric. Here we compare the results of applying several computerised structure prediction algorithms to the sequence of OmpG. Furthermore, we probe the OmpG topology by both an established chemical labelling approach and a new method which combines epitope insertion and surface plasmon resonance. The computational approaches are broadly accurate but the exact choice of the number of β strands remains difficult. The algorithms also tend to predict the entire β strand rather than just the transmembrane region. Epitope insertion clearly pinpoints exposed loops but its utility in defining buried or periplasmic sites is less clear cut. Cysteine-mutant labelling is largely confined to exposed residues but one periplasmic cysteine may be labelled by reagents entering via the OmpG pore.
© 2006 Published by Elsevier Inc.

Keywords: OmpG; Porin; Structure prediction; Surface plasmon resonance; Biotinylation; β-Barrel; Outer membrane

Bacterial outer-membrane proteins (OMP) mediate cell-environment interactions including nutrient uptake, adherence, and immunogenicity. Databases contain many hundreds of OMP sequences and, whilst solving their structures by X-ray crystallography is relatively successful, rapid predictions of structure are still important. Results of such structural predictions take the form of topology diagrams which define regions exposed to the surface, the membrane, and the periplasm [1,2]. Such information can then be used to design mutants, create surface display systems [3], raise peptide antibodies [4], or produce protein chimeras [5]. The architecture of OMP is fundamentally a β-barrel and the prediction methods seek to define this topology. Recently the structure of OmpG was solved [6] and as a water-filled monomeric pore it should provide a simple test for structure prediction. Structural predictions which try to detect hydrophobic moments of protein regions which divide polar protein interiors and the non-polar membrane should work best with such a water filled pore [2,7]. Similarly, the absence of monomer–monomer contacts should simplify computational and chemical methods. However the pore may allow chemical labels to enter the periplasm [8]. Here we examine the results of commonly used methods applied to the OmpG protein.

Materials and methods

Topology prediction. The membrane strand criterion combining hydrophobicity and hydrophobic moment was as defined in [2] and used the PRIFT hydrophobicity scale [9], *v* (the frequency of side chain rotation in the secondary structure) was 1/2 (straight β-sheet), and the window size used was 9 [2]. The method was programmed into a Microsoft Excel spreadsheet (Supplementary data). Turn prediction was performed as previously described [10]. The HMM prediction used the method of Martelli et al. [11] and was calculated online at (www.biocomp.unibo.it). DSSP analysis, according to Kabsch and Sander [12] used the online version at (bioweb.pasteur.fr/seqanal/interfaces/dssp-simple.html).

Protein engineering. OmpG (P76045) and its mutants were expressed in the outer membrane by the pMS119EH vector system and *Escherichia coli*

* Corresponding author. Fax: +441912227424.
E-mail address: j.h.lakey@ncl.ac.uk (J.H. Lakey).

0006-291X/$ - see front matter © 2006 Published by Elsevier Inc.
doi:10.1016/j.bbrc.2006.10.003

*BZB*1107 cells [4]. Site-directed mutagenesis, including Flag epitope insertion, was performed by QuikChange (Stratagene).

Topology testing using Flag-epitope insertions. Cells were grown at 37 °C to an OD_{600} of approximately 0.5 before induction by 1 mM isopropyl-β-D-thiogalactopyranoside (IPTG), followed by a further 1-h incubation to reach an approximate OD_{600} of 1.0. After equilibration for an hour on ice and two washes with phosphate-buffered saline (PBS), harvested cells were resuspended in PBS to give 5×10^9 cells/ml (OD_{600} of 1×10^9 cells/ml). For broken cell samples, cells were disrupted by a Branson tip sonicator (30 s on/30 s off for 10 min) on ice. For Western blot analysis of expression levels and proteolytic breakdown induced cells were boiled before loading onto the gel and visualisation was by ECL. Approximately equal amounts were loaded by always using the same cell density measured by OD_{600} (Fig. 2B).

Detection of Flag-epitope binding by surface plasmon resonance (SPR). Anti-Flag M2 monoclonal antibody (Sigma) was immobilised on flow cell 1 of CM-5 chips (Biacore) according to manufacturers instructions using a Biacore-X.

To study cell binding, 25 µl of intact or broken cell samples prepared as above was injected onto both flow cells, 240 s after the injection a wash with Hepes-buffered saline (HBS; 20 mM Hepes, 150 mM NaCl, and 3 mM EDTA, pH 7.5) was performed to eliminate non-specific binding. The chip was regenerated by washing with 8 µl of 10 mM NaOH. The flow rate was 5 µl/min throughout. Results shown (Fig. 2C) were corrected by subtracting the signal of the corresponding cell-free sample obtained by centrifugation at 11,000*g* for 30 min. Similarly, results presented in (Fig. 2D) have been corrected by subtracting the binding data of the corresponding membrane-free sample obtained by centrifugation at 125,000*g* for 30 min. This corrects for any soluble protein fragments containing Flag sequences.

Topology testing via single cysteine mutants: biotinylation of cysteine residues. Cysteine point replacement mutants were created in an OmpG expression plasmid in which a Flag epitope had previously been inserted in loop 6 (after I226). *E. coli* cells carrying these OmpG-Flag + cysteine mutants were prepared as follows: 3 ml of the induced cultures (see above) was harvested, and cells were washed once and finally resuspended in 1 ml of 0.2 M sodium phosphate buffer, 20% sucrose, and 5 mM $MgCl_2$ (pH 7) (buffer A). Then, biotin labelling was carried out using a modification of the protocol in [8] such that cells were incubated here with a 25-fold lower concentration (20 µM) of EZ-Link™ PEO maleimide activated biotin (Pierce) for 15 s. The reaction was quenched by a 1-min gentle agitation with 50 mM dithiothreitol (DTT), and samples washed twice with buffer A. Cell pellets were resuspended and boiled in 100 µl of 0.8% SDS. OmpG was immunoprecipitated from the resuspended solution by 5 µl of a 1:1000 dilution of ANTI-Flag® M2 monoclonal antibody in TBS (140 mM NaCl, 20 mM Tris, and 0.1% Tween 20, pH 8) saturated with an *E. coli* lysate. After 1-h incubation at 20 °C with agitation, 25 µl of Protein A–Sepharose 6 MB (Amersham) washed twice with TBS was added and incubated for 1 h at 20 °C with agitation. After being washed twice with TBS, the beads were boiled in SDS–PAGE sample buffer, resolved by SDS–PAGE, and transferred by semi-dry blotting onto a PVDF membrane. The membrane was blocked in Detector™ Block (KPL, USA), and then probed against a 1:10,000 dilution of ANTI-Flag® M2 monoclonal antibody, or Streptavidin–Peroxidase Polymer (Sigma) for 1 h. The membrane was extensively washed in TBS buffer. For detection of Flag, the blots were subjected to a final 1-h incubation with 1:20,000-diluted anti-mouse IgG (whole molecule) peroxidase-conjugated antibody (Sigma). Visualisation of the positive bands was carried out with ECL Plus Western Blotting Detection kit and Hyperfilm ECL (Amersham, UK).

Results and discussion

Topological predictions

The mean hydrophobicity, hydrophobic moment plus hydrophobicity (“membrane strand criterion”), turn prediction [2], and the positions of tryptophan and tyrosine residues are presented in Fig. 1 together with the

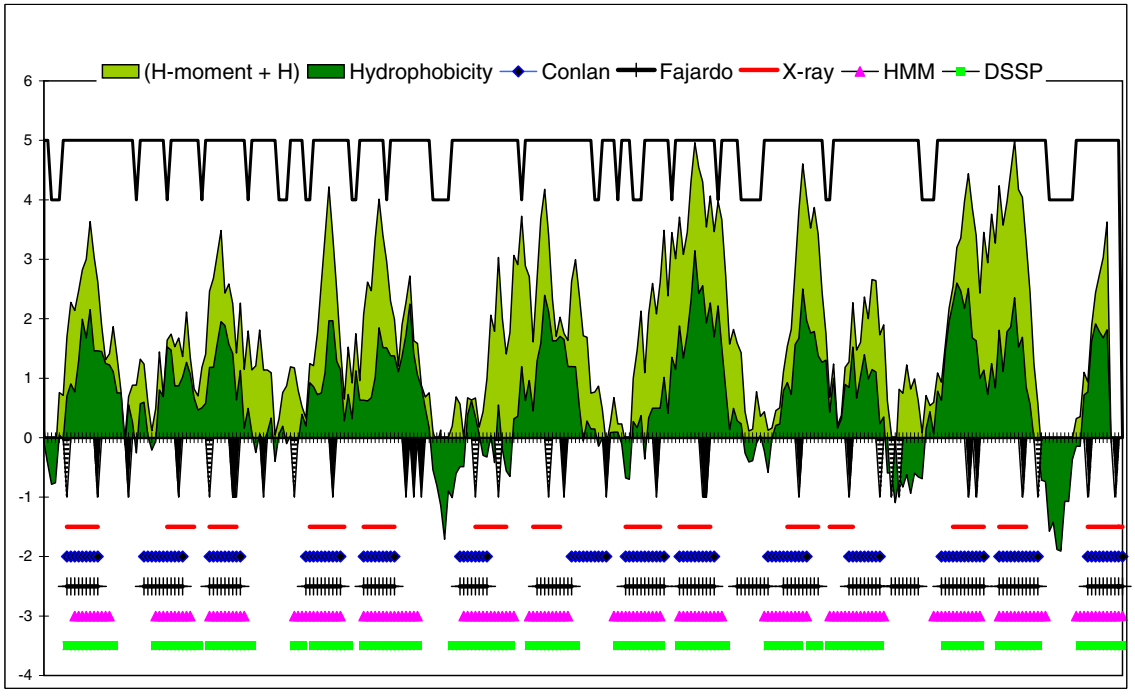

Fig. 1. OmpG topological prediction. Profiles of Membrane criteria (hydrophobic moment plus hydrophobicity; dark grey), mean hydrophobicity (light grey), turn prediction (Trough (=4) in upper line) [2], tyrosine (black), and tryptophan residue (stripes) as downward peaks below 0. Lower section; TM strands from X-ray structure, predictions by [13] and [14], and the HMM predictor [15] and finally β structure in the OmpG structure defined by DSSP analysis [12].

transmembrane strands previously predicted by Conlan [13] and Fajardo [14]; and the X-ray derived structure [6]. In addition, the results of the HMM-based predictor exclusively designed for outer-membrane β-barrel proteins [15] and a DSSP analysis [12] of the structure are shown (Fig. 1). The prediction of Conlan et al. [13], which used a combination of algorithms, correctly predicted 14 TM strands but by missing strand 7 shifted strands 2, 6, 10, and 11. Fajardo et al. are similar in the N-terminal half but, by predicting 17 strands, fit poorly towards the C-terminus [14]. The HMM-based predictor [15] is largely accurate and the membrane criteria method strongly matches a number of strands. However, both show a tendency to over-predict the strand length. The DSSP analysis, which defines β structure from the X-ray model, independent of membrane topology, shows that both these methods tend to predict the full β-strand rather than simply the TM segment (Fig. 1). Aromatic residues can help define TM regions and in OmpG the TM strand is often terminated by a tyrosine or tryptophan [1]. The tyrosines point away from the membrane core with their hydroxyl groups towards the polar interface. OmpG has more tryptophans (10) than are found in trimeric porins (2–4) [2]. Notably, those on strand ends are found further out from the membrane than the tyrosines and their indole rings point back towards the membrane core. Similar behavior occurs in OmpW [16], OmpA [17], and Tsx [18] monomeric Omp.

Topology probed by insertion of Flag epitopes

Six OmpG mutants were constructed with inserted Flag (DYKDDDDK) sequences after residues A59 (extracellular Loop 2 Flag, L2F), E79 (periplasmic Turn 3 Flag, T3F), W112 (Strand 6 Flag, S6F), S133 (S7F), T143 (L4F), and I226 (L6F). In addition the Loop 6 Flag (L6F) mutant was further modified. In one case the entire strand W43–Y50 was replaced by the Flag-like but non-binding "YQS" sequence (YQSDDDDK) to give ΔS3Y. In another, the YQS sequence was inserted in the same site as the Flag-sequence in S7F to give S7Y. This was used to test whether the insertion in S7F affects OmpG folding. (Mutations are displayed in Fig. 2A.) The expression levels of all the mutants were checked by Western blot to ensure that the altered binding to the mutants resulted from different epitope exposure and not different expression levels (Fig. 2B).

When cells expressing the mutant OmpG were tested for binding to anti-Flag mAb by SPR, the mutants L2F, L4F, and L6F, whose epitopes had been placed in the external loops, were recognised by the immobilised antibody (Fig. 2C). In contrast, the intact T3F cell, where the epitope was inserted in a periplasmic turn, showed no binding. Replacement of a whole transmembrane strand with the "YQS" sequence in the ΔS3Y mutant caused a significant decrease in the extracellular recognition of the Flag epitope presented in the loop L6. Thus the drastic replacement of a transmembrane strand by a hydrophilic sequence either

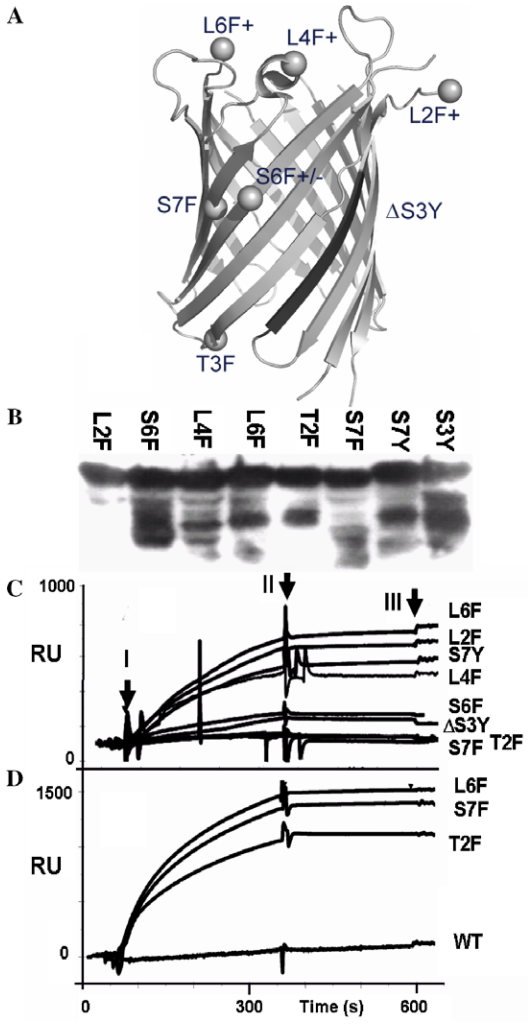

Fig. 2. Probing of the OmpG topology by insertion of Flag epitopes. (A) Position of residues preceding Flag insertions on the OmpG structure (PDB;2F1C) [6] with eventual SPR binding results indicated by + or ±. Substituted strand (ΔS3Y) shown in black. (B) A Western blot of the Flag-inserted mutants using anti-Flag. OmpG band is uppermost and lower bands indicate proteolytic breakdown products. (C,D) SPR detection of Flag epitope binding on an anti-Flag-immobilised chip in the intact- and disrupted-cell experiments, respectively. Flow rate = 5 μl/min. Roman numerals indicate sample injection starts (I); the injection end and start of 240-s wash delay (II); wash to eliminate non-specific binding (III).

causes the mutant protein to adopt a new conformation, in which L6 is not fully exposed, or that the replacement may inhibit the membrane assembly. The Western blot result (Fig. 2B) shows that the level of proteolytic degradation of ΔS3Y is among the highest, and hence the strand replacement inhibited OmpG assembly in the outer membrane.

Two mutants, S6F and S7F, tested the effect of inserting Flag into transmembrane strand-surface loop boundaries. The former is inserted at the beginning (N-terminus) of a strand and the latter at the end (C-terminus), each on the extracellular side. The binding to S6F was low and to S7F was like WT. To understand this lack of response we examined the mutant S7Y (non-binding Flag like

sequence). Here a similar sequence is inserted at residue 133 but the antibody response comes from a fully exposed Flag epitope concurrently located at L6. This mutant shows strong binding, similar to L6F and L2F, indicating that the low binding of S7F is not due to incorrect folding and membrane assembly. This is confirmed upon cell breakage, which was expected to expose only T2F, but also increased the binding of S7F to almost L6F levels. Thus epitopes inserted at the interface may not be well exposed [19], and their exposure can be sterically hindered by other cell-surface structures (e.g., LPS) [20]. S6F shows significantly higher degradation levels which may mean that folding is also inhibited. It was not tested by sonication. Recognition of an epitope in intact cells is therefore a good indication of clear exposure at the tips of surface loops. However, although sonication correctly exposed T2F it cannot be used as an indicator of periplasmic exposure since it also caused exposure of the previously hidden S7F.

Topology probed via biotinylated-cysteine mutants

Compared to epitope insertion this is a less structurally disruptive method since only a single residue is replaced by mutation [8]. The following OmpG positions were mutated L47C (Strand 3), W65C (Loop 2), V99C (Loop 3), W112C (Loop 3–Strand 6 interface), V120C (Strand 7–Loop 4 interface), L126C (Turn 3–Strand 7 interface), M134C (Strand 7–Loop 4 interface), and L141C (Loop 4–3_{10} helix) (Fig. 3A). As shown in Fig. 3C, mutants that were biotinylated in intact cells are W65C, V99C, W112C, V120C, and L141C while L47C, L126C, and M134C were not labelled. Labelling of L6F (no cysteine) was also performed as a negative control. KdgM, used previously [8], is assumed to form a smaller channel than OmpG [8] and it is more likely that the maleimide–biotin molecule can enter the OmpG pore and react with exposed cysteine residues.

The expression levels were also checked and although variable (Fig. 3B), the different protein concentrations did not relate to differences in the biotinylation levels. Although neither the biotinylation blot nor the anti-Flag blot is sufficiently quantitative to allow useful comparison of the band densities between the gels, in lanes where no biotinylation has occurred the anti-Flag blot clearly shows that the mutant protein is present.

The pattern of biotinylation shown in Fig. 3A and C does show a trend towards defining surface exposed residues such as 65, 99, and 141. Of the similar residues 47, 134, and 112 only the latter is labelled and although this correlates with a marginally greater surface exposure it does not help topology predictions. Most unexpectedly the residue 120 is strongly labelled whereas its neighbour 126 is not. The label may have penetrated the OmpG pore

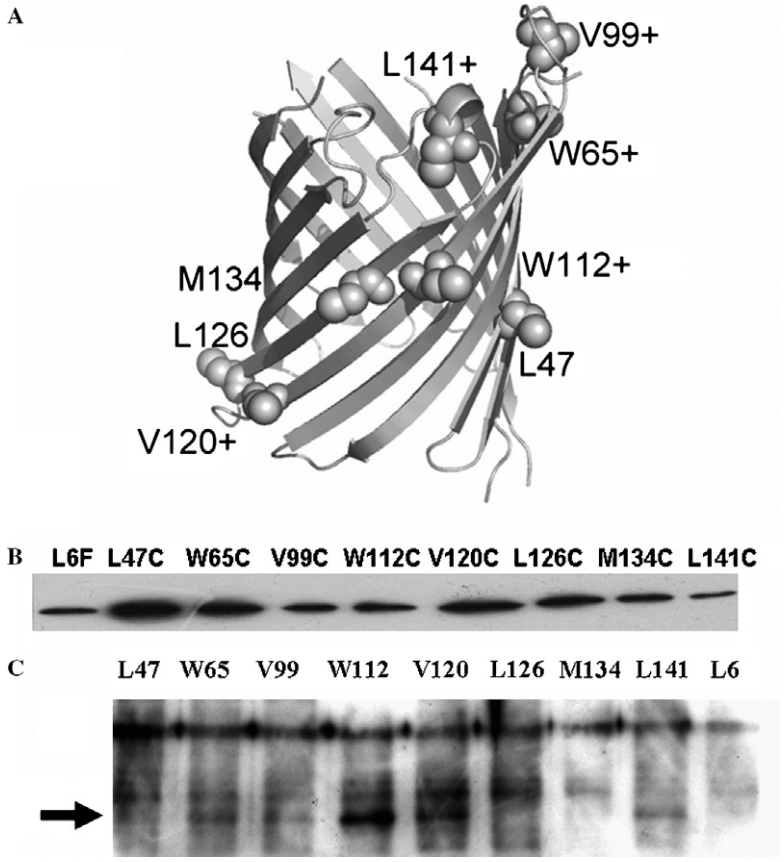

Fig. 3. Probing the OmpG topology using biotinylated cysteine mutants. (A) Cysteine mutants modelled on OmpG X-ray structure(PDB;2F1C) [6]. (+) indicates residues biotinylated in intact cells. (B,C) Western blots to detect the Flag epitope and biotinylation from the intact cell samples, respectively. The arrow in (C) indicates the position of the biotinylated OmpG band. The origin of the consistent band higher up the gel is unknown.

to reach residue 120 but the lack of binding to the similar 126 is not explained. Finally, the strongest labelling was observed not for the most exposed residues but for the two which are possibly interfacial. It may be that the amphipathic character of the label could concentrate it in this area and encourage this behavior.

In conclusion, the analysis of the OmpG structure has revealed specific limitations in current methods to predict the structures of β-barrel membrane proteins. The computational methods show that it is difficult to delineate the membrane-buried regions accurately. The positions of aromatic residues may yet be the key. Inserted epitopes can clearly be used in combination with the Biacore to detect the exposed ends of loops in intact cells. However, this method cannot be used with disrupted cells to define intracellular loops in sonicated samples. Specific disruption of a β-strand worked well and reduced the yield of folded protein significantly. Finally, although labelling of cysteines was generally successful, one internal residue was strongly labelled and would therefore have misled any prediction.

Acknowledgments

The authors wish to thank the Wellcome Trust (Equipment Grant 48873) and BBSRC for financial support. V.V. thanks the Royal Thai Government for a studentship and J.H.L. thanks the BBSRC for a Research Development Fellowship. We thank Helen Ridley for excellent technical assistance and Guy Condemine for helpful advice on biotinylation.

Appendix A. Supplementary data

Supplementary data associated with this article can be found, in the online version, at doi:10.1016/j.bbrc.2006.10.003.

References

[1] T. Schirmer, S.W. Cowan, Prediction of membrane-spanning beta-strands and its application to maltoporin, Protein Sci. 2 (1993) 1361–1363.
[2] D. Jeanteur, J.H. Lakey, F. Pattus, The bacterial porin superfamily: sequence alignment and structure prediction, Mol. Microbiol. 5 (1991) 2153–2164.
[3] H. Lang, Outer membrane proteins as surface display systems, Int. J. Med. Microbiol. 290 (2000) 579–585.
[4] G. Bainbridge, H. Mobasheri, G.A. Armstrong, E.J.A. Lea, J.H. Lakey, Voltage gating of *Escherichia coli* porin; a cystine scanning mutagenesis study of loop 3, J. Mol. Biol. 275 (1998) 171–176.
[5] C. Hikita, Y. Satake, H. Yamada, T. Mizuno, S. Mizushima, Structural and functional-characterization of the Ompf and Ompc porins of the *Escherichia coli* outer-membrane—studies involving chimeric proteins, Res. Microbiol. 140 (1989) 177–190.
[6] G.V. Subbarao, B. van den Berg, Crystal structure of the monomeric porin OmpG, J. Mol. Biol. 360 (2006) 750–759.
[7] J. Finer-Moore, R.M. Stroud, Amphipathic analysis and possible formation of the ion channel in an acetylcholine receptor, Proc. Nat. Acad. Sci. USA 81 (1984) 155–159.
[8] T. Pellinen, H. Ahlfors, N. Blot, G. Condemine, Topology of the *Erwinia chrysanthemi* oligogalacturonate porin KdgM, Biochem. J. 372 (2003) 329–334.
[9] J.L. Cornette, K.B. Cease, H. Margalit, J.L. Spouge, J.A. Berzofsky, C. DeLisi, Hydrophobicity scales and computational techniques for detecting amphipathic structures in proteins, J. Mol. Biol. 195 (1987) 659–685.
[10] C. Paul, J.P. Rosenbusch, Folding patterns of porin and bacteriorhodopsin, EMBO J. 4 (1985) 1593–1597.
[11] P.L. Martelli, P. Fariselli, G. Tasco, R. Casadio, The prediction of membrane protein structure and genome structural annotation, Comp. Funct. Genom. 4 (2003) 406–409.
[12] W. Kabsch, C. Sander, Dictionary of protein secondary structure—pattern-recognition of hydrogen-bonded and geometrical features, Biopolymers 22 (1983) 2577–2637.
[13] S. Conlan, Y. Zhang, S. Cheley, H. Bayley, Biochemical and biophysical characterization of OmpG: a monomeric porin, Biochemistry 39 (2000) 11845–11854.
[14] D.A. Fajardo, J. Cheung, C. Ito, E. Sugawara, H. Nikaido, R. Misra, Biochemistry and regulation of a novel *Escherichia coli* K-12 porin protein, OmpG, which produces unusually large channels, J. Bacteriol. 180 (1998) 4452–4459.
[15] P.L. Martelli, P. Fariselli, A. Krogh, R. Casadio, A sequence-profile-based HMM for predicting and discriminating beta barrel membrane proteins, Bioinformatics 18 (Suppl. 1) (2002) S46–S53.
[16] H.D. Hong, D.R. Patel, L.K. Tamm, B. van den Berg, The outer membrane protein OmpW forms an eight-stranded beta-barrel with a hydrophobic channel, J. Biol. Chem. 281 (2006) 7568–7577.
[17] A. Pautsch, G.E. Schulz, High-resolution structure of the OmpA membrane domain, J. Mol. Biol. 298 (2000) 273–282.
[18] J.Q. Ye, B. van den Berg, Crystal structure of the bacterial nucleoside transporter Tsx, EMBO J. 23 (2004) 3187–3195.
[19] A. Sukhan, R.E.W. Hancock, Insertion mutagenesis of the *Pseudomonas aeruginosa* phosphate-specific porin Oprp, J. Bacteriol. 177 (1995) 4914–4920.
[20] C.K. Murphy, V.I. Kalve, P.E. Klebba, Surface topology of the *Escherichia coli* K-12 ferric enterobactin receptor, J. Bacteriol. 172 (1990) 2736–2746.